Problems in Approximating Shapes of Planar Contours

Leif Ellingson* Chalani Prematilake†

Abstract

This paper is concerned with approximation problems involved in the similarity shape analysis of planar contours. Contours in this context may be thought of as the ranges of simple closed curves. While contours are by their very nature infinite-dimensional, in order for computations to be performed with digital images, discretization is unavoidable and results in some amount of approximation error. To aid in the quantification of this error, we use a polygonal approximation for the contours by evaluating the contours at k times. We explore methods for determining a rough lower bound for k and illustrate them using some examples.

Key Words: Shape analysis, discretization, approximation, planar curves

1. Introduction

The area of shape analysis in its modern form began with Kendall (1984), which mathematically defined the notion of direct similarity shape for finite-dimensional planar configurations. Such a configuration is traditionally represented as a k-ad, which is a set of k ordered, labelled points of interest called landmarks. Two k-ads $\mathbf{z_1} = (z_1^1, \ldots, z_1^k), \mathbf{z_2} = (z_2^1, \ldots, z_2^k) \in \mathbb{C}^k$ are said to have the same direct similarity shape, if there is a direct similarity S of the complex plane,

$$S(z) = wz + b, w \in \mathbb{C}^*, b \in \mathbb{C}$$

such that $S(z_1^j) = z_2^j, \forall j = 1, \ldots, k$. In other words, if $\mathbf{z_1}$ and $\mathbf{z_2}$ have the same direct similarity shape, they may differ only by translation, rotation, and scale.

The mathematical definition of direct similarity shape is thus defined as follows. Translations are filtered out by centering the k-ad $\mathbf{z} = (z^1, \ldots, z^k)$ to

$$\boldsymbol{\zeta} = (\zeta^1, \ldots, \zeta^k)$$
$$\zeta^j = z^j - \overline{z}, \forall j = 1, \ldots, k.$$

Unfortunately, rotation and scale are not so easily filtered out. Instead, the direct similarity shape, or Kendall shape of $\boldsymbol{\zeta}$ is defined using an equivalence class. Indeed, the Kendall shape $[\boldsymbol{\zeta}]$ of $\boldsymbol{\zeta}$ is the orbit under rotation and scaling of $\boldsymbol{\zeta}$. That is,

$$[\boldsymbol{\zeta}] = \{\lambda e^{i\theta}\boldsymbol{\zeta} : -\pi < \theta \leq \pi, \lambda > 0\}, \tag{1}$$

where λ is a scaling factor and θ is an angle of rotation about the origin.

As a result, the four configurations shown in Figure 1, despite differing from each other, all have the same Kendall shape. By virtue of this definition, shape data can be more difficult to work with quantitatively than standard multivariate data. Indeed, the space of all such shapes, denoted by Σ_2^k, can be identified with a projective space, meaning that traditional statistical techniques for Euclidean data cannot be directly used. Instead, data analysis requires the use of statistical techniques defined for use on manifolds.

*Department of Mathematics and Statistics, Texas Tech University, Lubbock, TX
†Department of Mathematics and Statistics, Texas Tech University, Lubbock, TX

For information regarding parametric and semi-parametric statistics on manifolds, please see Watson (1983), Small (1996), Dryden and Mardia (1998), Kendall et al. (1999), Mardia and Jupp (2000), Shi et al. (2009), and Fletcher (2012), among others. Bhattacharya and Patrangenaru (2003, 2005) and, independently, Hendriks and Landsman (1998) developed theory and methodologies for nonparametric statistical analysis on manifolds.

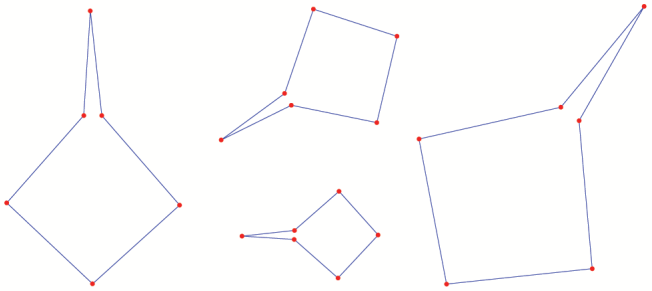

Figure 1: Four configurations that all have the same Kendall shape, differing only in rotation, translation, and scale from each other.

2. Landmark Selection

The statistical shape analysis of finite-dimensional planar configurations depends greatly upon the selection of the landmarks used to form the k-ads. As discussed in Dryden and Mardia (1998), landmarks are selected according to some set of rules, so as to both represent the object of interest well (for the purpose of the analysis) and achieve correspondence of landmarks across k-ads within a sample. Traditionally, a relatively small number of landmarks are selected either by an expert based upon anatomical features or according to mathematical features of interest, such as curvature, as shown in Figure 2 (middle). However, due to the amount of information lost by using only a small number of landmarks, as computing power has increased, researchers began to include equally spaced landmarks, often called pseudolandmarks, between those which were carefully selected, as in Figure 2 (right).

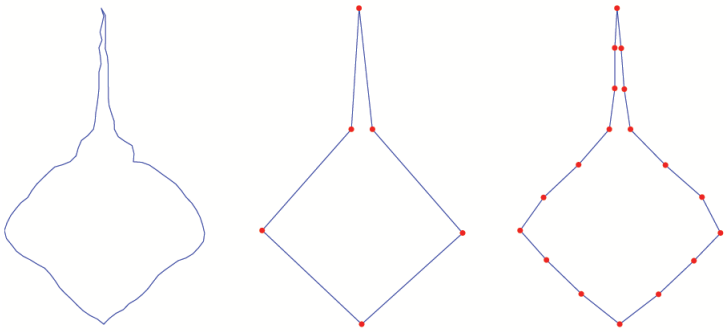

Figure 2: A contour of a stingray (left) represented as a k-ad using 6 carefully selected landmarks (middle) and with equally spaced pseudolandmarks placed between the original 6 landmarks (right).

Due to the rapid growth of imaging data available alongside the increase in computing power, many researchers have developed methods for automatic landmark selection when dealing with outlines of objects so as to speed up the data analysis process. Perhaps the most commonly used method is to systematically select equally spaced landmarks along

the outline of the object of interest, as mentioned above. Bookstein (1997) introduced semilandmarks, often referred to as sliding landmarks, which are found using thin-splate splines, and allow for the landmarks to move along the outline. Recently, Ellingson et al. (2013) introduced methodology for shapes of contours which is analogous to random landmark selection. Typically, methods such as these use values of k considerably larger than non-automated methods in order to allow the k-ads to well-represent the outline.

3. Similarity Shape of Planar Contours

Over the past 20 years, researchers have taken an interest in the analysis of shapes of curves, rather than finite-dimensional configurations. For instance, Grenander (1993) considered shapes as points on an infinite dimensional space. Furthermore, a manifold model for direct similarity shapes of planar closed curves, which was first suggested by Azencott (1994), was pursued in Azencott et al. (1996), and further detailed by Younes (1998, 1999).

This area gained additional ground the turn of the millennium, as more researchers began studying shapes of planar closed curves, as in Sebastian et al. (2003). Klassen et al. (2004), Michor and Mumford (2004), and Younes et al. (2008) follow the methods of Small (1996) and Kendall by defining a Riemannian structure on a shape manifold. Klassen et al. (2004) compute an intrinsic sample mean shape. subsequently, Mio and Srivastava (2004), Mio et al. (2007), Srivastava et al. (2005), Mio et al. (2005), Kaziska and Srivastava (2007), Joshi (2007), and, most recently, Kurtek et al. (2012) have explored the similarity shape of closed curves modulo reparametrizations for a chosen Riemannian metric.

However, we will consider the approach of Ellingson et al. (2013), which defines a contour $\tilde{\gamma}$ to be the range of a piecewise differentiable function γ that is parametrized by arclength:

$$\gamma : [0, L] \to \mathbb{C},$$

such that $\gamma(0) = \gamma(L)$ and γ is one-to-one on $[0, L)$. That is to say that the contour $\tilde{\gamma}$ is non-self-intersecting. Let z_γ denote the center of mass of γ. A contour $\tilde{\gamma}$ is said to be regular if γ is a simple closed curve, as defined above, and there is a unique point $z_0 = argmax_{z \in \tilde{\gamma}} \|z - z_{\tilde{\gamma}}\|$. In other words, there is a unique point on the contour that is furthest from the center of mass. For convenience, we will subsequently identify the contour with the function γ.

Just as in the the finite-dimensional case, the direct similarity shape $[\gamma]$ of a contour γ consists of all contours differing from γ by only rotation, translation, and/or scale. We can again filter out translations by centering the contour as follows:

$$\gamma_0 = \gamma - \bar{z}_\gamma = \{z - \bar{z}_\gamma, z \in \gamma\}.$$

γ_0 is called a centered contour. We say that two regular contours γ_1 and γ_2 have the same direct similarity shape if, for some non-zero complex number β, $\gamma_{2,0} = \beta\gamma_{1,0}$. More formally, we define the direct similarity shape of γ to be the orbit under rotation and scaling of γ_0. Symbolically, this can be expressed as:

$$[\gamma] = \{\lambda e^{i\theta}\gamma_0 : -\pi < \theta \leq \pi, \lambda > 0\},$$

where λ and θ are as defined in (1).

The closure of the complex vector space spanned by centered contours γ is a Hilbert space $\mathbf{H}$. As such, the set of all direct similarity shapes of regular contours Σ_2^{reg} is a dense and open subset of $P(\mathbf{H})$. Due to this, we again must appeal to the use of statistics on manifolds.

While there are a number of methods and metrics that could be used to analyze data lying on this space, we will conduct an extrinsic analysis. To do this, we must embed the shape space into an ambient Hilbert space in order to perform the statistical analysis. Here, we embed $P(\mathbf{H})$ in $\mathcal{L}_{HS} = \mathbf{H} \otimes \mathbf{H}$, the space of Hilbert-Schmidt operators of $\mathbf{H}$ into itself, via the Veronese-Whitney embedding j, which is given by

$$j([\gamma]) = \frac{1}{\|\gamma\|^2} \gamma \otimes \gamma,$$

where $[\gamma]$ denotes the shape of γ. The distance ρ induced via j is the Frobenius norm on the space of Hilbert-Schmidt operators. Let $A, B \in P(\mathbf{H})$. Then,

$$\rho^2(A, B) = \mathrm{Tr}\left((j(A) - j(B)) \otimes (j(A) - j(B))\right)$$

4. Discrete Approximations

Ideally, we could conduct data analysis directly using the preceding results, but when working with digital imaging data, it is necessary to discretize the data in some way. Since contours are functional data, we could appeal to techniques described in Ramsay and Silverman (2005) to approximate the contours using a finite number of basis functions of some kind. Another option is to approximate a contour as a k-ad and perform the analysis on Σ_2^{reg} using Σ_2^k, Kendall's shape space of finite planar configurations. If this were done, we would approximate each contour γ using a (centered) k-ad $\boldsymbol{\zeta}$ by selecting landmarks in some manner along the contour. We could then embed Σ_2^k into $S(k, \mathbb{C})$, the space of self-adjoint $k \times k$ complex matrices using the finite-dimensional Veronese-Whitney embedding given by $\frac{1}{\|\zeta\|^2} \zeta \zeta^*$.

However, while the problem of discretization is often mentioned, researchers often choose an arbitrary value for k despite the choice being non-trivial. It is important that the discrete approximation retains the features of the contour, so k must not be too low. On the other hand, for computational purposes, it is advantageous to not have too high of a value for k. As such, we would like to be able to find a rough lower bound for k for a given contour to find a balance between the competing factors described above.

Unfortunately, though, evaluating approximations can be tough using k-ads because there is a fundamental difference in nature between a finite-dimensional k-ad and an infinite-dimensional contour. Due to this, we want to discretize in a way that we can appeal to the finite-dimensional techniques while also remaining able to quantify approximation error.

4.1 Polygon Approximations

To solve this problem, Ellingson et al. (2013) proposed to approximate contours as polygons. To do this, sampling points are obtained by evaluating the contour γ at k times. The linear interpolation of the sampling points yields the k-gon z. It follows, then, that z is a one-to-one piecewise differentiable function that can be parametrized by arclength. As such, z can be evaluated at any number of times. Indeed, for $s \in (0, 1)$, the k-gon can be expressed as follows:

$$z(sL_k) = \begin{cases} (t_2 - sL_k)z(0) + sL_k z(t_2) & 0 < sL_k \leq t_2 \\ (t_j - sL_k)z(t_{j-1}) + (sL_k - t_{j-1})z(t_j) & t_{j-1} < sL_k \leq t_j \\ (L_k - sL_k)z(t_k) + (sL_k - t_k)z(0) & t_k < sL_k < L_k \end{cases}$$

for $j = 3, \ldots, k$. Here, L_k denotes the length of the k-gon, $z(t_j)$ is the jth ordered vertex, where $t_j \in [0, L_k)$, and $z(t_1) = z(0) = z(L_k)$.

The sampling points, which serve as vertices of the polygon (though some may be collinear), are analagous to landmarks and may be selected automatically, as discussed in Section 2. For the purposes of this paper, we are considering only sampling points equally spaced along the contour. It should also be noted that the center of mass of a k-gon may differ from that of a classical k-ad, though the difference is most profound for small k, as in Figure 3. However, as $k \to \infty$, the centers of mass for both types of configurations both converge to the center of mass of the contour.

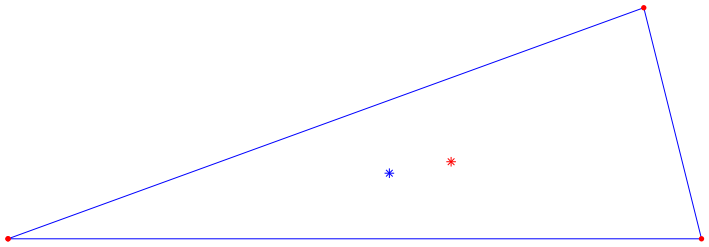

Figure 3: A triangle and its center of mass (blue) along with a 3-ad formed from the triangle's vertices and its center of mass (red)

4.2 Lower Bound Using Squared Distance in the Shape Space

Suppose that the digital image of the contour consists of K pixels. From (4.1), it follows that z can be evaluated at K times. Indeed, the space of direct similarity shapes of non-self-intersecting regular polygons is dense in the space of direct similarity shapes of regular contours. As a result, the contour and k-gon, along with their respective shapes, are objects in the same space as each other, allowing for approximation error to be evaluated directly.

Due to this, a natural choice for a criterion with which to find a lower bound for k might be based upon the distance ρ in the shape space. As an initial choice, we decided to explore using ρ^2. Out goal was to find the smallest value of k such that $\rho^2(z_k, \gamma_K) < 0.05$, where γ_K is the "best" approximation of γ available. We chose 0.05 as a cutoff with the interpretation of it being a 5% relative squared-distance with respect to γ_K since the norm of each shape is defined to be 1.

For a given contour, the algorithm we used to find a lower bound for k is as follows:

1. Evaluate γ at K times to obtain the "best" approximation γ_K.
2. Evaluate γ at k times to obtain z_k.
3. Calculate the squared distance $\rho^2(z_k, \gamma_K)$.

4. Repeat steps 2 and 3 for values of k between 4 and K.

5. Choose the smallest k such that $\rho^2(z_k, \gamma_K) < 0.05$.

As an example, this methodology was applied for a contour of a dog shown in Figure 4. Figure 5 displays the plot of ρ^2 versus k for this contour. Interestingly, ρ^2 decreases rapidly, falling below the chosen threshold at only 17 sampling points. The 17-gon, as is shown in Figure 4, captures the general form of the contour of the dog, but all of the details are missing, as would be expected for such a low-dimensional approximation. This suggests that ρ^2 may not be suitable as a criterion for choosing a lower bound for k.

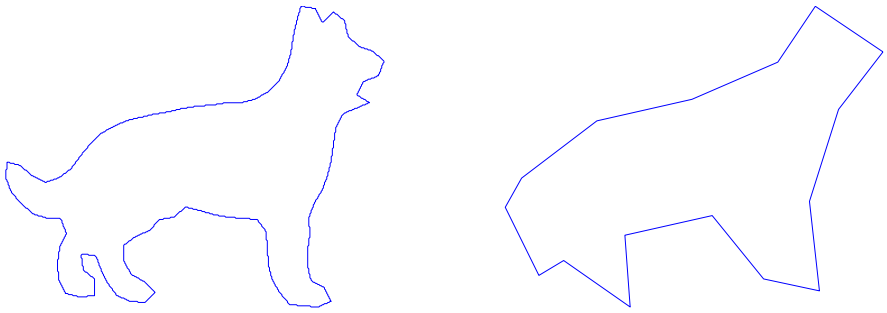

Figure 4: The contour of a dog (left) and the associated polygon approximation (right) obtained using ρ^2 to determine a lower bound for k.

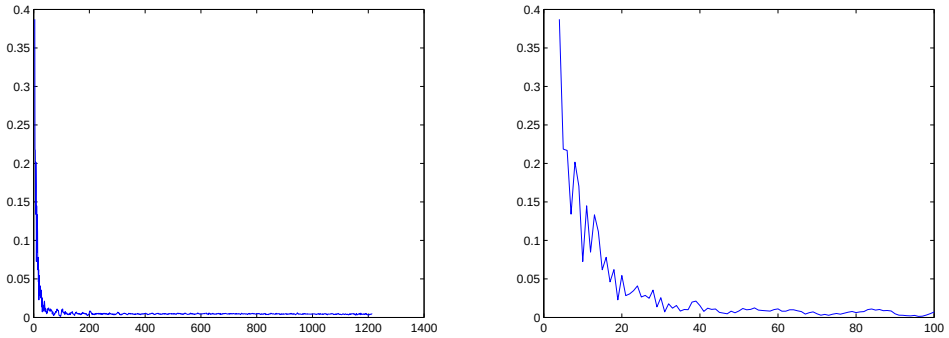

Figure 5: A plot of ρ^2 versus k for the contour of a dog for all values of k (left) and zoomed in for small values of k (right).

A second example using the contour of a stingray is shown in Figure 6. Similarly to the previous example, Figure 7 shows that ρ^2 decreases rapidly as k increases for small values of k. Indeed, here, our criterion suggests that only 18 sampling points are sufficient to approximate the shape of the contour. However, the 18-gon, as shown in Figure 6, self-intersects in the tail of the stingray because of the high amount of curvature in this region of the contour while also being incredibly narrow. As such, our approximation violates our requirements, providing further support for this criterion not being appropriate for finding a good lower bound for k.

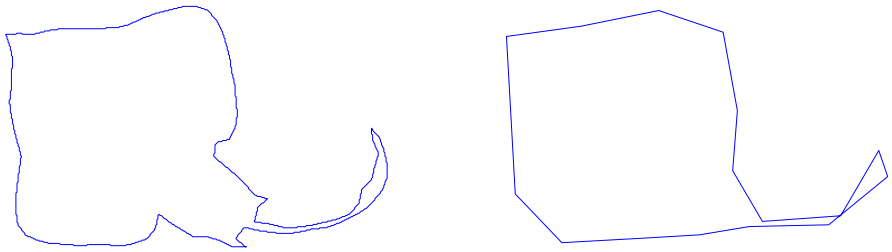

Figure 6: The contour of a stingray (left) and the associated polygon approximation (right) obtained using ρ^2 to determine a lower bound for k.

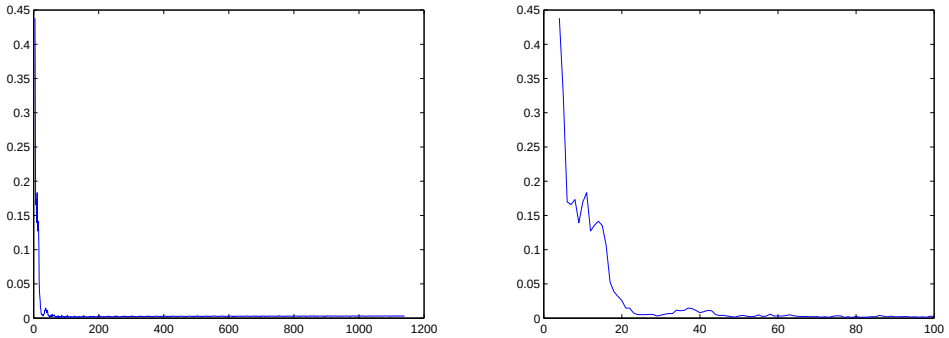

Figure 7: A plot of ρ^2 versus k for the contour of a stingray for all values of k (left) and zoomed in for small values of k (right).

4.3 Lower Bound Using Difference in Length

Motivated by the fact that using the squared distance in the shape space as a criterion for finding a lower bound for k produced approximations that were unsatisfactory, we decided to explore methods for approximating the contour, itself, instead of the shape. To do this, we appealed to the fact that, for a given contour, the lengths, or circumferences, of the polygon approximations are bounded above by the length of the contour. Furthermore, as k increases, the length of the k-gons converge to the upper bound. The length L_k for a given k-gon is

$$L_k = \sum_{j=2}^{k+1} \|z(t)_j - z(t_{j-1})\|,$$

where $z(t_{k+1}) = z(0)$. The length of γ_K can be calculated similarly and is denoted by L_K. As our cut-off criterion, we chose to use 5% relative error in lengths with respect to γ_K. For a given contour, the procedure we used to find a lower bound for k is as follows:

1. Compute L_K.
2. For some value k, compute L_k.
3. Compute the relative error of L_k compared to L_K.
4. Repeat steps 2 and 3 for values of k between 4 and K.

5. Choose the smallest k such that the $\frac{L_K - L_k}{L_K} < 0.05$.

To examine how this criterion works compared to ρ^2, we performed this procedure for the same two contours as previously used. For the contour of the dog, a plot of of $\frac{L_K - L_k}{L_K}$ versus k is shown in Figure 8. While the relative error quickly declines as k increases, the decrease is not as rapid as it was for ρ^2. As a result, the smallest values of k that satisfies our criterion is considerably higher. In fact, this criterion provides a lower bound of 473 sampling points. The resulting polygon approximation is shown alongside the original contour in Figure 9. Notice that, unlike in the previous scenario, there is no visual distinction between the contour and approximation. The plot of $\frac{L_K - L_k}{L_K}$ versus k for the contour of a stingray is

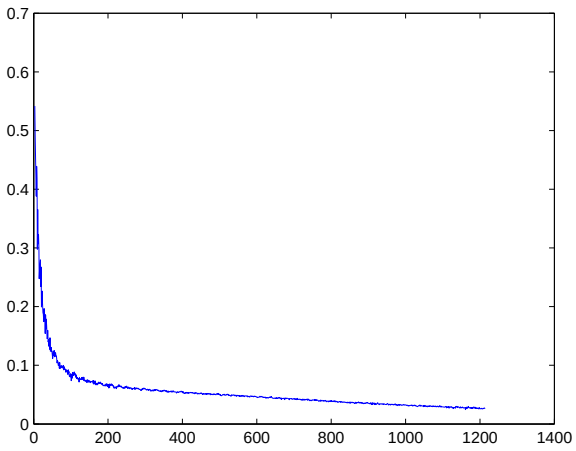

Figure 8: A plot of $\frac{L_K - L_k}{L_K}$ versus k for the contour of a dog for all values of k

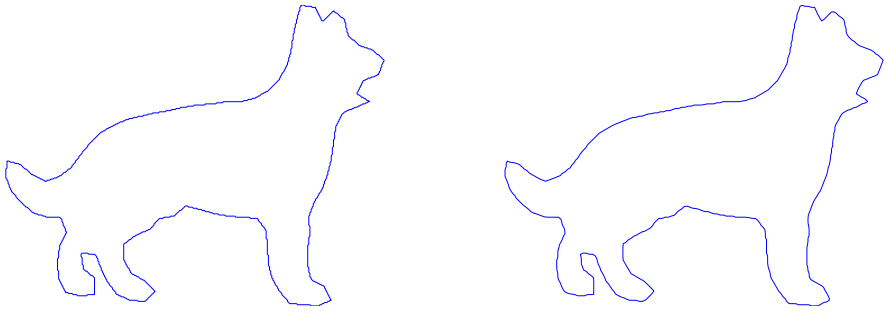

Figure 9: The contour of a dog (left) and the associated polygon approximation (right) obtained using $\frac{L_K - L_k}{L_K}$ to determine a lower bound for k.

shown in Figure 10. The lower bound for k using this criterion is 305 sampling points. The polygon approximation is shown beside the original contour in Figure 11. As with the contour of the dog, the approximation is visually nearly indistinguishable from the contour. Additionally, there is no problem with self-intersection using this criterion, unlike with the previous criterion.

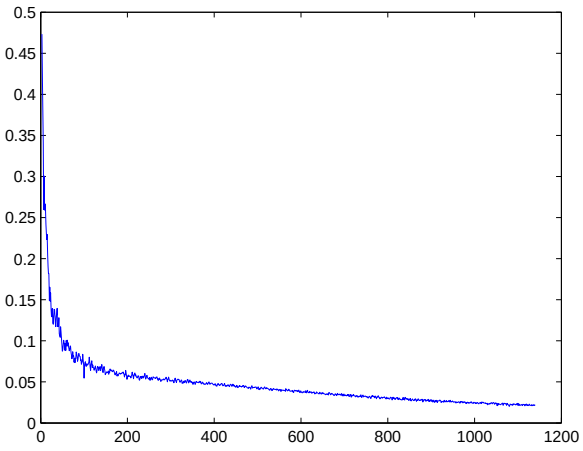

Figure 10: A plot of $\frac{L_K - L_k}{L_K}$ versus k for the contour of a stingray for all values of k

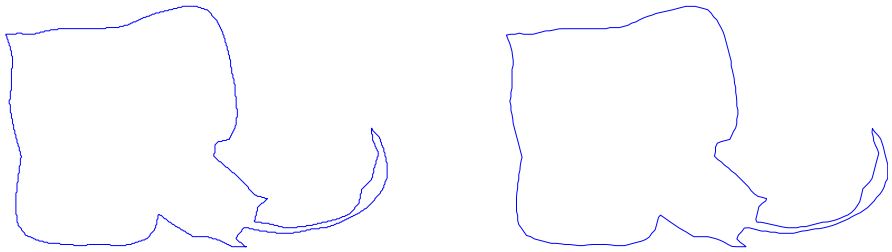

Figure 11: The contour of a stingray (left) and the associated polygon approximation (right) obtained using $\frac{L_K - L_k}{L_K}$ to determine a lower bound for k.

5. Conclusions

Based upon these computations, it appears that, of the two criteria explored here, the relative error in lengths produced a more conservative lower bound for k than the squared distance in the shape space did. As such, the polygon approximations using the more conservative lower bounds more closely visually resemble the contours. However, this results in these approximations requiring considerably more sampling points, increasing the effective dimensionality of the approximations and computational cost.

This result leads to the question of which is more important for a given application: analyzing the approximation of the shape of the contour or the shape of the approximation of the contour. If the former is suitable for a given problem, then using ρ^2 to determine a lower bound for k may suffice. However, if approximating the contour, itself, is important for the task at hand, then alternative methods comparing the contour and approximation as functions may be necessary.

Here, we suggest comparing the lengths of the functions, but this was merely an initial exploration to determine whether appealing to the configurations, themselves, rather than their shapes might be worth consideration. Since these preliminary results suggest that to be the case, further study appears to be warranted. Indeed, there are many techniques from functional data analysis that could be more appropriate than what we considered here.

Furthermore, for both criteria, our cut-off to determine a lower bound for k was chosen somewhat arbitrarily. Due to the scree-like nature of the plots of our criteria versus k, a more natural choice may be to use the bend in the plot. From the examples shown here, this change would seem to affect bounds found using the relative error in length more, as the bends in the plots occur near 10% rather than 5%.

Additionally, here we consider only approximating single observations. While this is certainly of use for gaining a better understanding of the problem, a more practical scenario is to consider problems when approximating a number of observations. Most notably, many problems in shape analysis involve calculating and estimating means, whether extrinsic or intrinsic. As such, an immediate extension is to apply the same ideas explored here to the approximation of sample means. Beyond that, it would be natural to explore the effect that the approximations have on estimation problems.

Acknowledgements

The authors would like to thank Vic Patrangenaru, Frits Ruymgaart, and Magdalena Toda for discussions on this and related projects.

References

[1] R. Azencott. (1994). Deterministic and random deformations ; applications to shape recognition. *Conference at HSSS workshop in Cortona, Italy.*

[2] R. Azencott and F. Coldefy and L. Younes. (1996). A distance for elastic matching in object recognition. *Proceedings of 12th ICPR* (1996), 687–691.

[3] R. N. Bhattacharya and V. Patrangenaru, (2003). Large sample theory of intrinsic and extrinsic sample means on manifolds-Part I, *Ann. Statist.* **31**, no. 1, 1-29.

[4] R. N. Bhattacharya and V. Patrangenaru. (2005). Large sample theory of intrinsic and extrinsic sample means on manifolds- Part II, *Ann. Statist.*, **33**, No. 3, 1211- 1245.

[5] F. L. Bookstein (1997) Landmark methods for forms without landmarks: morphometrics of group differences in outline shape. *Med Image Anal.* **1**(3), p. 225-43.

[6] I. Dryden and K. Mardia. (1998) Statistical Shape Analysis. Wiley: Chichester.

[7] L. Ellingson, V. Patrangenaru, and F. Ruymgaart. (2013). Nonparametric Estimation of Means on Hilbert Manifolds and Extrinsic Analysis of Mean Shapes of Contours. *Journal of Multivariate Analysis.* **122**, 317-333.

[8] P. T. Fletcher. (2012). Geodesic Regression and the Theory of Least Squares on Riemannian Manifolds. *International Journal of Computer Vision*. doi: 10.1007/s11263-012-0591-y

[9] U. Grenander (1993). *General Pattern Theory.* Oxford Univ. Press.

[10] H. Hendriks and Z. Landsman (1998). Mean Location and Sample Mean Location on Manifolds: Asymptotics, Tests, Confidence Regions. *Journal of Multivariate Analysis*, **67**, No. 2, p. 227-243.

[11] S. Joshi, A. Srivastava, E. Klassen, and I. Jermyn. (2007). Removing Shape-Preserving Transformations in Square-Root Elastic (SRE) Framework for Shape Analysis of Curves. *EMMCVPR*. August.

[12] D. Kendall, D. Barden, T. Carne, and H. Le. (1999). Shape and Shape Theory. Wiley, New York.

[13] J. T. Kent. (1992), New directions in shape analysis. *The Art of Statistical Science, A Tribute to G.S. Watson*, 115–127. Wiley Ser. Probab. Math. Statist. Probab. Math. Statist., Wiley, Chichester, 1992.

[14] E. Klassen, A. Srivastava, W. Mio, and S. H. Joshi. (2004). Analysis of Planar Shapes Using Geodesic Paths on Shape Spaces, IEEE PAMI **26** 372 - 383.

[15] S. Kurtek, A. Srivastava, E. Klassen, Z. Ding. (2012). Statistical Modeling of Curves Using Shapes and Related Features, Journal of the American Statistical Association, Accepted for Publication.

[16] K. Mardia and P. Jupp. (2000) Directional Statistics.

[17] P. W. Michor and D. Mumford. (2004). Riemannian Geometries on Spaces of Plane Curves. *Journal of the European Mathematical Society*, **8**, 1 - 48.

[18] W. Mio and A. Srivastava. (2004). Elastic-String Models for Representation and Analysis of Planar Shapes. *Proceedings of the IEEE Computer Society International Conference on CVPR*.10–15.

[19] W. Mio, A. Srivastava and E. Klassen. (2004)Interpolation by Elastica in Euclidean Spaces.*Quarterly of Applied Math.* **62**, 359 - 378 .

[20] W. Mio, A. Srivastava, and S. Joshi. (2007). On the Shape of Plane Elastic Curves. *International Journal of Computer Vision*, **73**, 307–324.

[21] T. B. Sebastian, P. N. Klein, and B. B. Kimia. (2003). On Aligning Curves. *IEEE Trans. Pattern Analysis and Machine Intelligence* **25**, no. 1, 116–125.

[22] X. Shi, M. Styner, J. Lieberman, J. Ibrahim, W. Lin, and H. Zhu. (2009). Intrinsic regression models for manifold-valued data. *Med Image Comput Comput Assist Interv.* 12 (Pt 2), p. 192-9.

[23] C. G. Small. (1996). The Statistical Theory of Shape. Springer-Verlag, New York.

[24] A. Srivastava, S. Joshi, W. Mio, and X. Liu. (2005). Statistical Shape Analysis: Clustering, Learning and Testing. *IEEE Trans. Pattern Analysis and Machine Intelligence*, **27**. 590–602.

[25] G. S. Watson. (1983). Statistics on Spheres. University of Arkansas Lecture Notes in the Mathematical Sciences. Wiley, New York.

[26] L. Younes. (1998). Computable elastic distance between shapes. *SIAM Journal of Applied Mathematics*, **58**, 565-586.

[27] L. Younes (1999). Optimal matching between shapes via elastic deformations. *Journal of Image and Vision Computing*, **17**, 381-389.

[28] L. Younes, P. W. Michor, J. Shah and D. Mumford (2008). A metric on shape space with explicit geodesics. *Rend. Lincei Mat. Appl.* **19** 25-57.